

## Featured Article

# Induction of Thyroid Cancer Cell Apoptosis by a Novel Nuclear Factor $\kappa$ B Inhibitor, Dehydroxymethylepoxyquinomicin

Dmitriy V. Starenki,<sup>1</sup> Hiroyuki Namba,<sup>1</sup>  
Vladimir A. Saenko,<sup>2</sup> Akira Ohtsuru,<sup>4</sup>  
Shigeto Maeda,<sup>3</sup> Kazuo Umezawa,<sup>5</sup> and  
Shunichi Yamashita<sup>1,2</sup>

<sup>1</sup>Department of Molecular Medicine, Atomic Bomb Disease Institute, and <sup>2</sup>Department of International Health and Radiation Research, Nagasaki University Graduate School of Biomedical Sciences, Nagasaki, Japan; <sup>3</sup>Division of Endocrine Surgery, and <sup>4</sup>Takashi Nagai Memorial International Hibakusha Medical Center, Nagasaki University Hospital, Nagasaki, Japan; and <sup>5</sup>Department of Applied Chemistry, Faculty of Science and Technology, Keio University, Yokohama, Japan

## ABSTRACT

**Purpose:** The objective of the study was to determine the effects of a novel selective nuclear factor  $\kappa$ B (NF- $\kappa$ B) inhibitor, dehydroxymethylepoxyquinomicin (DHMEQ), in thyroid carcinoma cells *in vitro* and *in vivo* and to additionally elucidate the molecular mechanisms underlying the action of this chemotherapeutic agent.

**Experimental Design:** In the *in vitro* experiments, the induction of apoptosis by DHMEQ in various human thyroid carcinoma cell types was determined by flow cytometry analysis of annexin-V binding and the caspase activation by Western blotting. For the *in vivo* study, female nu/nu mice were xenografted with s.c. FRO thyroid tumors. DHMEQ solution was injected i.p. at a dose of 8 mg/kg/day for two weeks. Tumor dimensions were monitored twice weekly, and apoptosis in tumor specimens was determined by terminal deoxynucleotidyl transferase-mediated nick end labeling staining.

**Results:** Treatment with DHMEQ substantially inhibited the translocation of p65 and p50 NF- $\kappa$ B subunits to the nucleus, the DNA-binding activity of the RelA/p65, NF- $\kappa$ B-dependent expression of the inhibitor of apoptosis (IAP)-family proteins, cIAP-1, cIAP-2, and XIAP, and the *de novo*

synthesis of inhibitor of nuclear factor  $\kappa$ B  $\alpha$ . At concentrations ranging from 0.1 to 5  $\mu$ g/ml, DHMEQ induced a caspase-mediated apoptotic response that could be abrogated by the c-Jun NH<sub>2</sub>-terminal kinase inhibitor SP600125 but not by either mitogen-activated protein/extracellular signal-regulated kinase kinase or p38 inhibitors. In contrast, normal human thyrocytes were resistant to DHMEQ-induced apoptosis. At higher doses of DHMEQ we observed the necrotic-like killing of both normal and malignant thyrocytes, which was resistant to mitogen-activated protein kinase inhibitors. In nude mice DHMEQ substantially inhibited tumor growth without observable side effects, and increased numbers of apoptotic cells were observed in the histologic sections of tumors treated with DHMEQ.

**Conclusions:** Our results show the potential usefulness of the novel NF- $\kappa$ B inhibitor, DHMEQ, in future therapeutic strategies for the treatment of thyroid cancers that do not respond to conventional approaches.

## INTRODUCTION

Nuclear factor- $\kappa$ B (NF- $\kappa$ B) is a key regulator of genes involved in the control of cellular proliferation and apoptosis (1). In most cases, activation of NF- $\kappa$ B protects against cell death by up-regulation of antiapoptotic factors such as TRAF, inhibitor of apoptosis (IAP), p21, and Bcl-XL (2, 3), and basal NF- $\kappa$ B activity is often increased in various types of human hematopoietic and solid tumors (4). Persistent NF- $\kappa$ B activity can be a result of either chromosomal amplification, overexpression, and rearrangement of genes coding for Rel/NF- $\kappa$ B factors, constitutive activation of upstream signaling kinases, or mutations inactivating inhibitory inhibitor of nuclear factor  $\kappa$ B (I $\kappa$ B) subunits. It is generally believed that the NF- $\kappa$ B-induced factors promote apoptotic resistance, transformation, cell growth, metastasis, and angiogenesis in neoplastic tissues (5), and cell survival in some cancer types, such as hematologic malignancies, clearly depend on NF- $\kappa$ B (6). Hence, the inhibition of NF- $\kappa$ B activity is an intuitive approach to cancer therapy and has broad appeal, such that it has now been attempted in a variety of cancer types (7, 8).

In thyroid cancers, NF- $\kappa$ B also plays an important role, and its signaling pathways are impaired through the mechanism of sustained activation, which contributes to the malignant potential of anaplastic thyroid carcinoma (ATC) cell lines. Inhibition of RelA/p65 protein synthesis with specific antisense oligonucleotides has been shown to greatly reduce the ability of two ATC cell lines to form colonies in soft agar, and their growth rate was also inhibited *in vitro* (9). Additionally, the inhibition of radiation-induced activation of the NF- $\kappa$ B cascade potentiated the proapoptotic effect of radiation therapy in inoculated ATC tumors *in vivo* (10). Thus, the apoptosis-permissive effects

Received 3/8/04; revised 7/6/04; accepted 7/12/04.

**Grant support:** Grant-in-Aid for General Scientific Research from the Ministry of Education, Science, Sports, and Culture of Japan (15590981, H. Namba; 14380256, V. Saenko; and 15390295 and 15659223, S. Yamashita).

The costs of publication of this article were defrayed in part by the payment of page charges. This article must therefore be hereby marked *advertisement* in accordance with 18 U.S.C. Section 1734 solely to indicate this fact.

**Requests for reprints:** Hiroyuki Namba, Department of Molecular Medicine, Atomic Bomb Disease Institute, Nagasaki University Graduate School of Biomedical Sciences, 1-12-4 Sakamoto, Nagasaki 852-8523, Japan. Phone: 81-95-849-7116; Fax: 81-95-849-7117; E-mail: namba@net.nagasaki-u.ac.jp.

©2004 American Association for Cancer Research.

of a NF- $\kappa$ B blockade can be considered as a promising strategy for the treatment of ATC.

A novel NF- $\kappa$ B inhibitor, dehydroxymethylepoxyquinomicin (DHMEQ) is a derivative of the antibiotic epoxyquinomicin C (11) and has been found to inhibit tumor necrosis factor (TNF)- $\alpha$  induced activation of NF- $\kappa$ B by suppressing NF- $\kappa$ B nuclear translocation (12). This drug promotes apoptosis in various cancer cell types and has been shown to be effective against rheumatoid arthritis, bladder cancer, and hormone-refractory prostate cancer in an *in vivo* model without apparent toxic side effects (13, 14). The present study was set up to determine the effects of DHMEQ in thyroid carcinoma cells both *in vitro* and *in vivo* and to additionally elucidate the molecular mechanisms underlying the action of this chemotherapeutic agent.

## MATERIALS AND METHODS

**Reagents.** Stock solutions of racemic DHMEQ (10 mg/ml) were prepared in DMSO and stored at  $-20^{\circ}\text{C}$ . TNF- $\alpha$  was purchased from WAKO (Osaka, Japan) and prepared at stock concentrations of 10  $\mu\text{g}/\text{ml}$  in water, then stored at  $-20^{\circ}\text{C}$ . The c-Jun NH<sub>2</sub>-terminal kinase (JNK) inhibitor SP600125 and the p38 mitogen-activated protein kinase inhibitor (p38 MAPK inhibitor here and hereafter) were purchased from Calbiochem (La Jolla, CA), dissolved in DMSO at stock concentrations of 20 mmol/L and 10 mmol/L, respectively, and then stored at  $-20^{\circ}\text{C}$ . The mitogen-activated protein/extracellular signal-regulated kinase kinase (MEK)1 inhibitor PD98059 (Cell Signaling, Beverly, MA) was dissolved in DMSO at a stock concentration of 10 mmol/L and stored at  $-20^{\circ}\text{C}$ . Antibodies were obtained from the following sources: anti-p50 polyclonal, p65 polyclonal, Bcl-xL polyclonal, and Bcl-2 monoclonal from Santa Cruz Biotechnology (Santa Cruz, CA); I $\kappa$ B $\alpha$  polyclonal, X-linked inhibitor of apoptosis (XIAP) polyclonal, poly(ADP-ribose) polymerase (PARP) polyclonal, cleaved caspase antibody kit, phospho-Erk1/2 pathway kit, phospho-stress-activate protein kinase (SAPK)/JNK pathway kit, antirabbit IgG, and antimouse IgG horseradish peroxidase-conjugated secondary antibody from Cell Signaling; and cIAP-1 polyclonal and cIAP-2 polyclonal from R&D Systems (Minneapolis, MN).

**Cell Culture.** Human anaplastic thyroid carcinoma cell lines FRO and ARO, papillary carcinoma cell line TPC-1, and the follicular carcinoma cell line WRO were initially provided by James A. Fagin (University of Cincinnati College of Medicine, Cincinnati, OH). The papillary carcinoma cell line KTC-1 and the anaplastic carcinoma cell line KTC-2 were a gift from Junichi Kurebayashi (Kawasaki Medical School, Kurashiki, Japan; refs. 15, 16). Cell lines were grown in RPMI 1640 supplemented with 5% fetal bovine serum and 1% (w/v) penicillin/streptomycin in a 5% CO<sub>2</sub> humidified atmosphere at  $37^{\circ}\text{C}$ . Primary human thyroid cell culture was established as described previously (17) and maintained in a DMEM:F12 (1:2) mixture supplemented with 3% fetal bovine serum and 1% (w/v) penicillin/streptomycin [all of the reagents were obtained from Sigma (St. Louis, MO)].

### Preparation of Cell Extracts and Immunoblotting.

Cells were washed twice with ice-cold PBS, collected in 1 ml PBS, and centrifuged for 3 minutes at 3,000 rpm. For total cell

extracts, each pellet was resuspended in 200  $\mu\text{L}$  of lysis buffer (Cell Signaling) containing protease and phosphatase inhibitors. After 15 minutes on ice, lysates were centrifuged for 15 minutes at 15,000 rpm at  $4^{\circ}\text{C}$ , and the supernatants were stored at  $-80^{\circ}\text{C}$ . Nuclear extracts were prepared as described previously (18). Protein concentrations were determined with a Bichinonic acid assay kit (Sigma). For Western blotting analysis, proteins were resolved by SDS-PAGE, transferred onto polyvinylidene difluoride membranes (Millipore, Bedford, MA), and subjected to immunoblotting with appropriate primary and secondary antibodies. Complexes were visualized with enhanced chemiluminescence reagents (Amersham, Arlington Heights, IL).

**DNA-Binding Assay.** The multiwell colorimetric assay for active NF- $\kappa$ B was done as described previously (19), with a *trans*-AM NF- $\kappa$ B p65 Transcription Factor Assay Kit (Active Motif North America, Carlsbad, CA), according to the manufacturer's instructions. Briefly, nuclear extracts (5  $\mu\text{g}$  of protein per well) were incubated in 96-well plates coated with immobilized oligonucleotide, containing a NF- $\kappa$ B consensus binding site. NF- $\kappa$ B binding to target oligonucleotides was detected by incubation of samples with primary antibodies against the p65 subunit provided with the kit. For quantification of activity, optical densities were measured at 450 nm with a microplate reader (ImmunoMini NJ-2300, System Instruments, Tokyo, Japan). Background binding levels measured by incubation with a mutant  $\kappa$ B probe provided in the kit was subtracted from the determined values.

**Cell Survival Assay.** Cultures were established in 96-well flat-bottomed microtiter plates (Nalge Nunc International, Tokyo, Japan). Cells were counted and resuspended in RPMI 1640 containing 5% FBS, and the suspensions (100  $\mu\text{L}$ , 2,000 cells/well) were added to each well and incubated for 24 hours before treatment. Solutions containing DHMEQ and inhibitors were added to each well in 10  $\mu\text{L}$  of medium at various concentrations, with 6 wells used for each concentration. In the control wells a solution of DMSO was added so that final concentration of DMSO in each well was 0.1%. After incubation, according to experimental protocols, a water-soluble tetrazolium salt-based assay was done as follows: 10  $\mu\text{L}$  of CKK-8 solution (Dojin, Osaka, Japan) were added to each well and incubated for 1 hour at  $37^{\circ}\text{C}$ . Optical densities were measured at 450 nm in a microplate reader.

**Flow Cytometry Analysis with the Annexin V/Propidium Iodide Assay.** Adherent cells were harvested by trypsinization and washed once with warm PBS. Cells ( $1 \times 10^5$ ) were double stained with FITC-conjugated annexin V and propidium iodide for 15 minutes at room temperature in a Ca<sup>2+</sup>-enriched binding buffer (apoptosis detection kit, Wako Chemicals, Osaka, Japan) then analyzed on a FACSCalibur flow cytometer (BDIS, Becton Dickinson, San Jose, CA). FITC and propidium iodide emissions were detected in the FL-1 and FL-2 channels, respectively. For each sample, data from 30,000 cells were recorded in list mode on logarithmic scales. Subsequent analysis was done with Cell Quest software (BDIS).

**Nude Mouse Xenograft Model.** All animal experiments described in this study were conducted in accordance with the principles and procedures outlined in the Guide for the Care and Use of Laboratory Animals of the Biomedical Research Center, Center for Frontier Life Science (Nagasaki University, Naga-

saki, Japan). FRO cells ( $5 \times 10^6$ ) resuspended in RPMI 1640 were injected s.c. into both flanks of 8-week-old female BALB/c nu/nu mice (Charles River Japan, Tokyo), 8 animals per group. Tumor sizes were measured each alternate day with calipers, and tumor volumes were calculated according to the formula  $a^2 \times b \times 0.4$ , where  $a$  is the smallest tumor diameter and  $b$  is the diameter perpendicular to  $a$ . DHMEQ, diluted in PBS to DMSO ratio (1:1), was injected i.p. at a dose of 8 mg/kg/day for two weeks, beginning from day 5 after tumor implantation. Animals from the control group received vehicle injections. Tumor size was then monitored for three more weeks for which the body weight, feeding behavior, and motor activity of each animal were used as indicators of general health.

**Histologic Estimation of Apoptosis in the Tumors.** Tumors were dissected, fixed in 10% neutral-buffered formalin, and embedded in paraffin. Apoptotic cells were detected in 5- $\mu$ m sections with an ApopTag Peroxidase Kit (Intergen Co., Burlington, MA). Positively stained cells were counted in four fields ( $\times 100$ ) for each specimen, and the apoptotic index was determined as the ratio of apoptotic cell number to total cell number.

**Statistical Analysis.** All data were expressed as the mean  $\pm$  SD. Differences between groups were examined for statistical significance with ANOVA and/or the Student's  $t$  test where appropriate. A  $P < 0.05$  indicated a statistically significant difference.

## RESULTS

### Cytotoxic Effects of DHMEQ in Thyroid Carcinoma Cells.

To determine the effect of DHMEQ on thyroid cancer cells, we used cultured human thyroid carcinoma cell lines established from follicular, papillary, and anaplastic thyroid tumors. Each of these cancer cell lines showed a decreased viability after treatment with DHMEQ at a dose range of 0.1 to 20  $\mu$ g/ml (Fig. 1A). At the highest DHMEQ dose concentrations, no living cells remained after incubation for 24 hours. In contrast, cultured primary thyrocytes showed substantially lower sensitivity to DHMEQ, and no effect on primary cell survival was observed until the DHMEQ dose was increased to 10  $\mu$ g/ml. At a concentration of 1  $\mu$ g/ml, DHMEQ inhibited the growth of anaplastic thyroid carcinoma cell lines in a time-dependent manner but exerted no effect on normal thyrocytes (Fig. 1B).

**Effects of DHMEQ on NF- $\kappa$ B Activation in Thyroid Cancer Cells.** To study the effect of DHMEQ on NF- $\kappa$ B activity, we did a DNA-binding assay with nuclear extracts from the ATC cell line, FRO, which has been previously shown to have elevated levels of constitutively active NF- $\kappa$ B (10). Cells were either exposed to X-rays or treated with TNF- $\alpha$  to activate the NF- $\kappa$ B cascade followed by an evaluation of NF- $\kappa$ B DNA binding. DHMEQ was found to suppress basal DNA binding of the p65 subunit in a dose-dependent manner and inhibit the activation of NF- $\kappa$ B by both ionizing radiation and TNF- $\alpha$  (Fig. 2A). As DHMEQ has been reported to interfere with the nuclear translocation of NF- $\kappa$ B, we studied the levels of p50 and p65 subunits in nuclear extracts of treated cells. After 2 hours incubation, DHMEQ decreased the nuclear content of both subunits in unstimulated cells and prevented TNF- $\alpha$ -induced

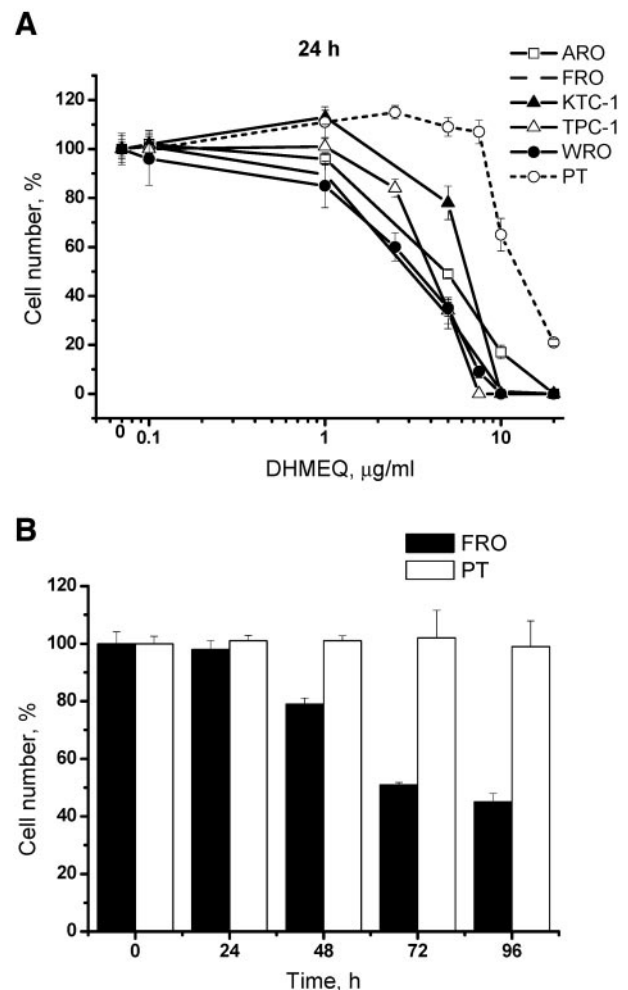


**Fig. 1** Cytotoxic effects of DHMEQ in human thyroid carcinoma cell lines and normal thyrocytes. **A**, Cells were treated with various concentrations of DHMEQ and incubated for 24 hours. **B**, viability of transformed and normal thyrocytes after treatment with 1  $\mu$ g/ml DHMEQ during 0 to 96 hours. Cell growth was estimated by water-soluble tetrazolium salt-based assays in 96-well plates. Bars, mean  $\pm$  SD. (PT, primary thyrocytes)

accumulation of the NF- $\kappa$ B subunits (Fig. 2B). DHMEQ, at a dose of 10  $\mu$ g/ml, also induced the degradation of cytoplasmic I $\kappa$ B $\alpha$ , which was detectable 2 to 4 hours after drug administration (Fig. 2C). NF- $\kappa$ B is known to bind the I $\kappa$ B promoter and activate its synthesis (20) and, therefore, the inhibition of NF- $\kappa$ B by DHMEQ probably suppressed *de novo* synthesis of I $\kappa$ B $\alpha$ . However, after longer incubation with DHMEQ, I $\kappa$ B $\alpha$  protein expression was restored to normal levels, which may be explained by both drug degradation and/or a recovery of the NF- $\kappa$ B signaling as has been reported previously (13).

As a result of treatment with DHMEQ, and most probably because of NF- $\kappa$ B inhibition, we also observed a decrease in the cellular levels of the IAP family proteins, cIAP-1, cIAP-2, and XIAP (Fig. 2D), the expression of which is known to be regulated by this transcription complex (21). The expression level of an antiapoptotic protein Bcl-xL, which also has a  $\kappa$ B binding

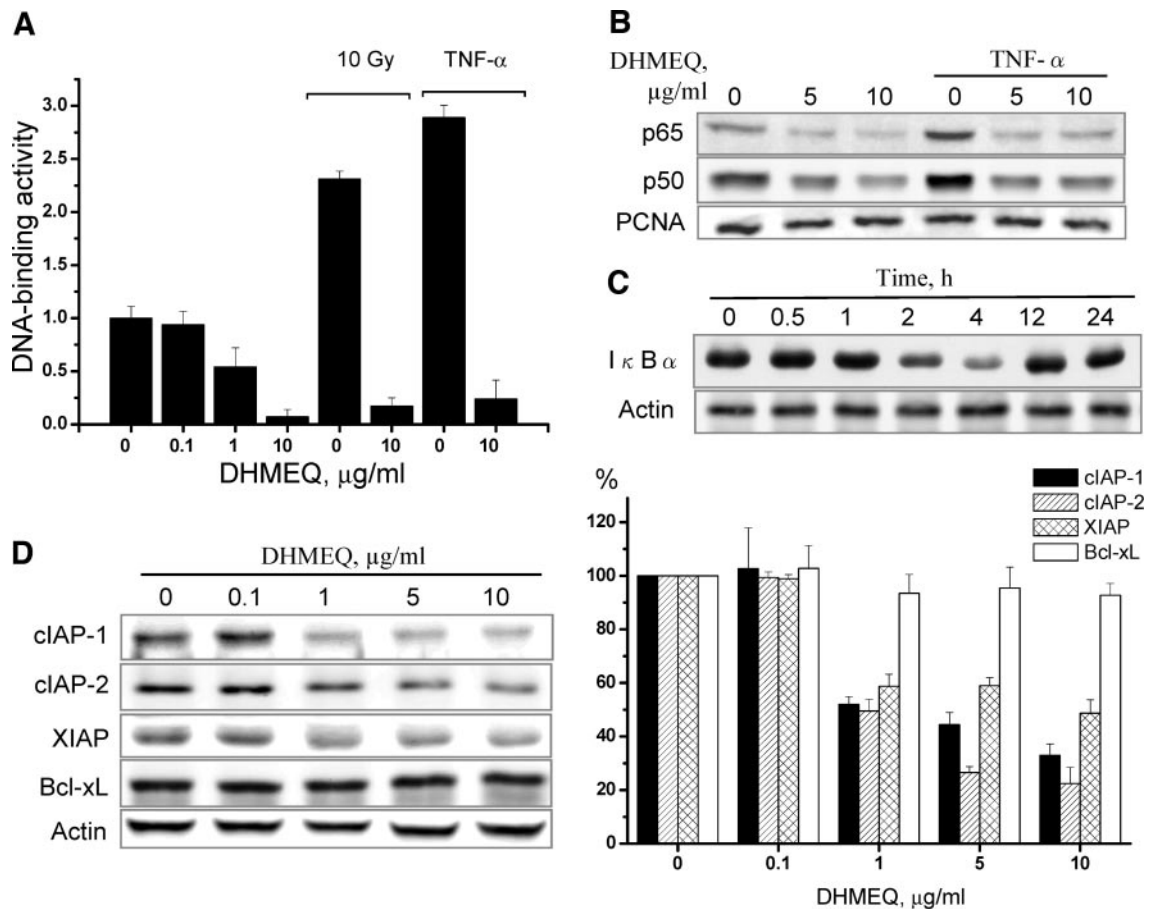


**Fig. 2** Effect of DHMEQ on NF- $\kappa$ B activation in the FRO cell line. **A**, DHMEQ inhibits both basal and induced p65 DNA-binding activity. One hour after pretreatment with DHMEQ, cells were either treated with 10 ng/ml TNF- $\alpha$  or exposed to 10 Gy of X-rays and incubated for 1 hour. Nuclear extracts were isolated from cultured cells, and binding assays were done as described in Material and Methods. **B**, inhibition of the nuclear translocation of NF- $\kappa$ B subunits. Cells were pretreated with various doses of DHMEQ for 1 hour then incubated with 10 ng/ml TNF- $\alpha$  for 1 hour. Western blotting was done with antibodies against p65 and p50. **C**, effects of DHMEQ on I $\kappa$ B $\alpha$  protein levels. Cell lysates were collected at different time points of incubation with 5  $\mu$ g/ml DHMEQ. **D**, down-regulation of IAP family and Bcl-xL protein levels by DHMEQ. Cells were incubated with various doses of DHMEQ for 24 hours, then total cell lysates were analyzed by Western blotting. The densitometry plot is shown to the right of the Western blots. Data are of three experiments. Bars, mean  $\pm$  SD.

site in its gene promoter (22), decreased insignificantly even after the treatment with high doses of DHMEQ.

**Apoptotic Changes in DHMEQ-Treated Thyroid Cancer Cells.** To assess the capability of thyroid carcinoma cells to undergo apoptosis in response to drug exposure and to help distinguish between different types of cell death, DHMEQ-treated cells were double stained with annexin V and propidium iodide and analyzed by flow cytometry. Significant numbers of apoptotic cells were induced by DHMEQ at a range of dose concentrations from 0.1 to 10  $\mu$ g/ml (Fig. 3A). An additional increase in DHMEQ concentrations caused an accumulation of propidium iodide<sup>+</sup> cells, indicating either that the integrity of the plasma membrane is being compromised or that propidium iodide excretion machinery is suppressed. At increasing doses of DHMEQ, we also detected a simultaneous increase in both the annexin V<sup>+</sup>/propidium iodide<sup>-</sup> fraction (early apoptotic) and annexin V<sup>+</sup>/propidium iodide<sup>+</sup> (regarded as necrotic) subpopulations (Fig. 3B). The induction of necrosis by high doses of

DHMEQ clearly contrasts with the typical apoptotic response, evaluated by FACS analysis, after exposure of the cells to 10 J/m<sup>2</sup> of UV radiation. DHMEQ induced the accumulation of annexin V-positive cells in two other thyroid anaplastic carcinoma cell lines, ARO and KTC-2 (Fig. 3C). In all of the cases, we also observed the rapid elevation of propidium iodide<sup>+</sup> fractions with the increase of DHMEQ doses (data not shown).

#### Effects of DHMEQ on Procaspase and PARP Cleavage.

Induction of apoptosis by DHMEQ was additionally characterized by examining the cleavage of procaspases. DHMEQ triggered procaspase and caspase substrate PARP cleavage in ATC cells (Fig. 4A), and the activation of caspases was detected within a wide dose range, from 0.1  $\mu$ g/ml to a maximal dosage of 10  $\mu$ g/ml (at which point no attached cells remained in the dishes). Consistent with the annexin V/propidium iodide assay data, the intensity of apoptotic procaspase and PARP cleavage was maximal between drug concentration levels of 0.1 and 1  $\mu$ g/ml. At higher concentrations, a marked decrease in active

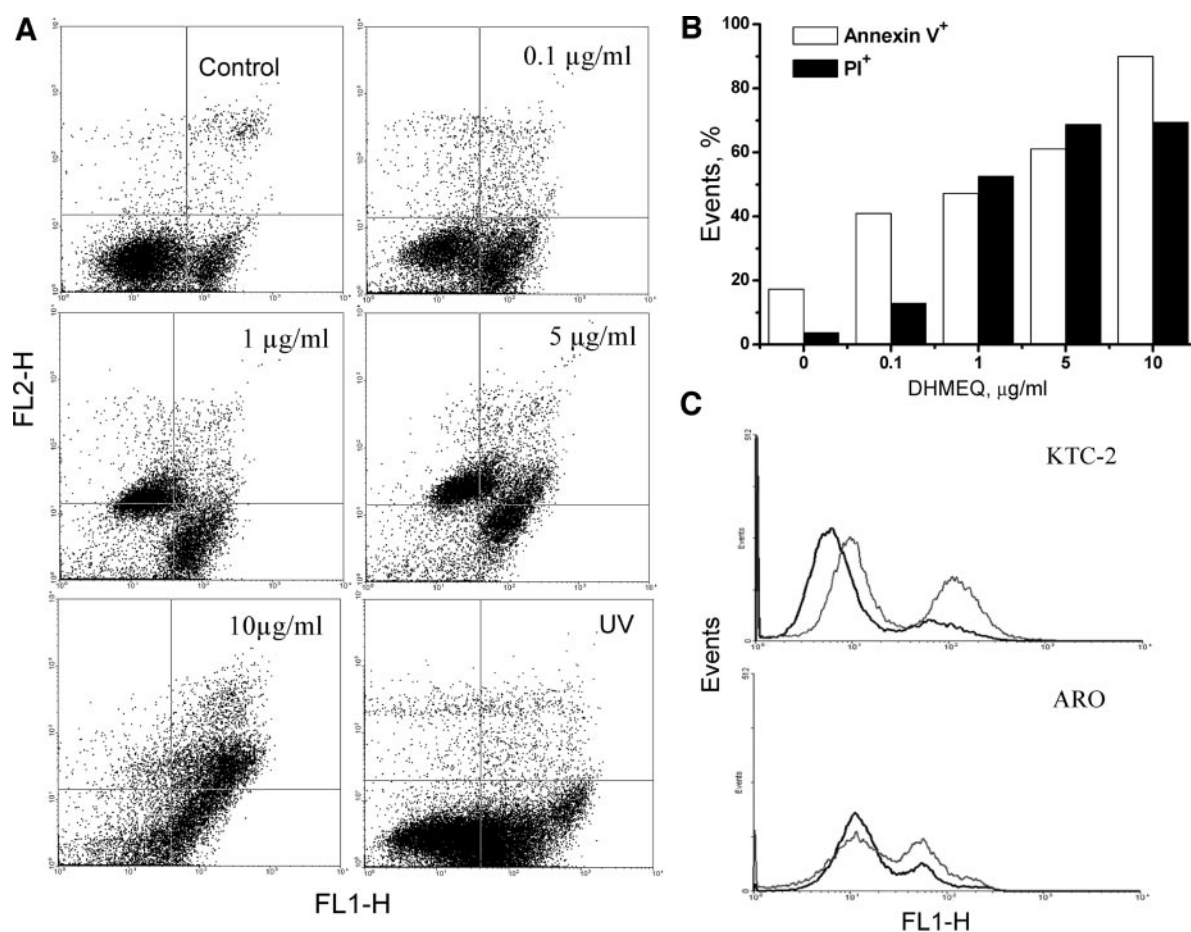


**Fig. 3** Apoptotic changes in DHMEQ-treated thyroid cancer cells. *A* and *B*, Annexin V/propidium iodide staining and FACS analyses were done to quantify phosphatidylserine externalization and advanced stage of cell death in FRO cells either treated with a range of DHMEQ doses for 24 hours or exposed to UV ( $10 \text{ J/m}^2$ ). The percentage of annexin V-positive cells is the sum of the events in the UR and LR quadrants and the percentage of propidium iodide-positive cells is a sum of the events in the top left and top right quadrants. *C*, Cultured anaplastic thyroid carcinoma cell lines, KTC-2 and ARO, were incubated with  $1 \mu\text{g/ml}$  DHMEQ for 24 hours, then double-stained with annexin V and propidium iodide, and analyzed by FACS. The histograms represent the increase in annexin V-positive fractions in DHMEQ-treated cells (□) compared with the untreated control (■).

caspase and cleaved PARP fragments was observed. Together with effector caspase-3 and -6, DHMEQ also activated the cleavage of the upstream procaspase-9, indicating the initiation of the mitochondrial apoptotic pathway. These findings correlate with the observed release of cytochrome *c* from the mitochondria to the cytoplasm (data not shown). DHMEQ-treated cells also displayed manifestations of caspase-8 activation, a key effector of death receptor-triggered apoptosis (23). It has also been shown that procaspase-8 can be a substrate for caspase-3, as part of an apoptosis amplification loop, after initiation of the cytochrome *c*/caspase-9 pathway (24). In a time course experiment, both procaspase and PARP cleavage products first appeared after 12 hours of incubation (data not shown). In contrast to carcinoma cell lines, DHMEQ did not induce cleavage of procaspases or PARP in primary thyrocytes (Fig. 4*B*). Although DHMEQ (at a concentration  $20 \mu\text{g/ml}$ ) induced 100% cell death after 24 hours incubation, no traces of active forms of caspases were detected.

**Activation of MAPK Cascades in DHMEQ-Treated Cancer Cells.** MAPK pathways have been implicated in the modulation of apoptotic cell death in response to chemotherapy (25). It has also been shown that activation of the extracellular signal-regulated kinase (ERK) pathway is linked to cell proliferation and survival, whereas induction of the stress-activated kinases, JNK and p38, is associated with increased apoptosis (26). In any event, both the extent and duration of MAPK signaling have been shown to be critical for the determination of cell fate (27). Therefore, we examined the time course effect of DHMEQ on different MAPK pathways, which are possible mediators of apoptosis. We found that DHMEQ enhanced the phosphorylation of ERK, p38, JNK-1, and JNK-2 in transformed thyrocytes within a short time after treatment (Fig. 5). ERK activation was transient and peaked at 2 to 8 hours, after which time its phosphorylation levels returned to baseline at 24 hours after treatment. Analysis of the phosphorylation of JNK and p38 revealed a sustained pattern of phosphorylation level

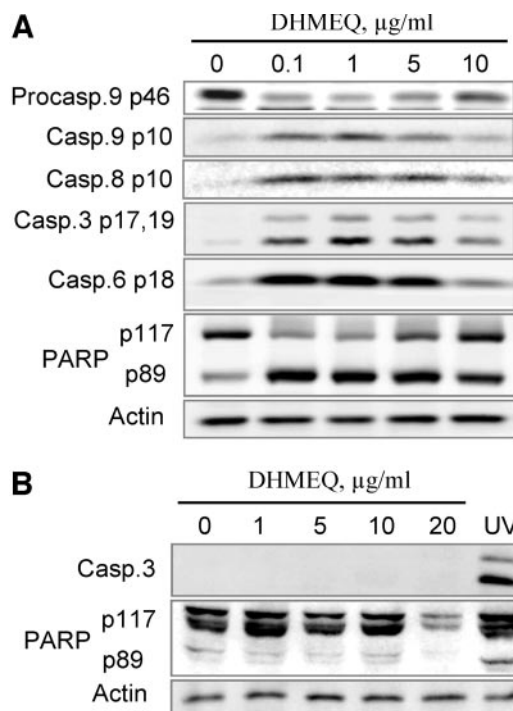


**Fig. 4** Effects of DHMEQ on procaspase and PARP cleavage in an ATC cell line, FRO (A), and in normal thyrocytes (B). Cells were treated with the indicated doses of DHMEQ for 24 hours. Exposure to UV (10 J/m<sup>2</sup>) was used as a positive control for the apoptotic effects in primary thyrocytes. Procasp, procaspase; Casp, caspase.

increases during the 24-hour observation interval, and this was initially detectable 30 minutes after drug administration. Treatment with DHMEQ, however, did not change the expression levels of ERK, JNK, and p38.

**Effect of Inhibitors of the MAPK Family on DHMEQ Cytotoxicity.** To additionally assess the relevance of the observed MAPK pathway activation to the effects of DHMEQ, we investigated whether the inhibition of MAPK pathways modulates cell survival after treatment. To analyze individual MAPK signaling cascades, we used specific inhibitors of MEK (PD98059), p38 (p38 MAPK inhibitor), and JNK (SP600125). We found that neither the inhibition of MEK nor that of p38 had any detectable effect on thyroid carcinoma cell viability after treatment with DHMEQ (Fig. 6A). In contrast, however, incubation with SP600125 suppressed DHMEQ cytotoxicity in each of the cell lines tested. In addition, a profound cell rescue effect was observed for the JNK inhibitor at DHMEQ dose range of 0.1  $\mu\text{g/ml}$  to 5  $\mu\text{g/ml}$  (Fig. 6A), but at higher concentrations of DHMEQ, JNK inhibition could not prevent cell death. Analysis of caspase cascade activation revealed that SP600125 also inhibited DHMEQ-induced activation of the upstream caspases-8 and -9, cleavage/activation of the effector caspase-3, and subsequent PARP cleavage (Fig. 6B). Neither MEK nor p38 inhibition has any such effects despite efficient inhibition of their respective kinases (data not shown).

**In vivo Effects of DHMEQ.** DHMEQ has been reported to suppress the *in vivo* growth of inoculated hormone-refractory

prostate cancer (13). To examine the effects of DHMEQ in model ATC xenografts *in vivo*, we used nude mice with implanted FRO tumors. A substantial delay in tumor growth rate was detected in mice who received a solution of DHMEQ *i.p.* for two weeks, although treatment with DHMEQ did not prevent the development of tumors (Fig. 7A). After dissecting these tumors, we analyzed their morphology and determined the prevalence of apoptotic cells. The number of terminal deoxynucleotidyl transferase-mediated nick end labeling (TUNEL)-positive cells in histologic slides of tumor tissues from DHMEQ-treated mice was higher than in control animals (Fig. 7B). During the course of therapy no changes in the behavior of animals were observed. To additionally evaluate the drug toxicity, we also examined the morphologic structure and manifestations of apoptosis in small intestine epithelium of treated animals. No changes on histology or increased numbers of TUNEL-positive cells were found in the specimens compared with controls (data not shown).

## DISCUSSION

The transcriptional factor NF- $\kappa$ B and the Rel/NF- $\kappa$ B signaling pathway are implicated in the regulation of cellular proliferation, apoptotic response, and oncogenesis. The elevation of basal levels of the NF- $\kappa$ B activity in malignant thyroid tissue plays a critical role in thyroid carcinogenesis, which makes NF- $\kappa$ B an attractive target for molecular therapy. In a previous report, we showed that inhibition of NF- $\kappa$ B signaling in anaplastic thyroid cancer cells markedly suppressed the tumor growth *in vivo* (10). Therefore, we supposed that NF- $\kappa$ B-targeted therapy could potentially result in advances in a successful treatment of advanced thyroid cancers. However, until recently, no effective small molecule compound was available to selectively inhibit the NF- $\kappa$ B cascade. The development of DHMEQ and its effective application *in vivo* led us to investigate the effect of this new drug in thyroid cancer. In the current study,

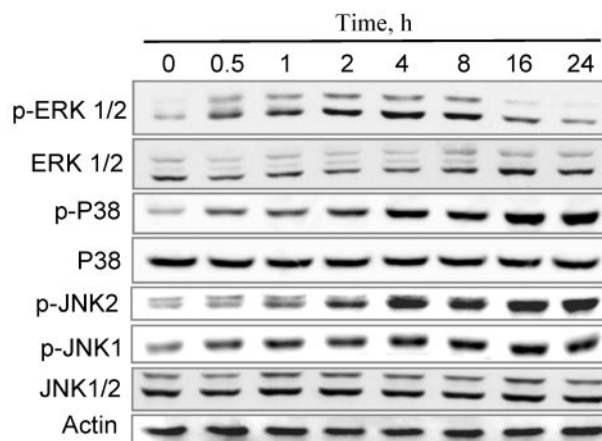


**Fig. 5** Activation of MAPK cascades in DHMEQ-treated thyroid cancer cells. FRO cell lysates were collected at different time points of incubation with 5  $\mu\text{g/ml}$  DHMEQ. Western blotting was done with antibodies specific to the nonphosphorylated and phosphorylated forms of the corresponding proteins. ERK, extracellular signal-regulated kinase.

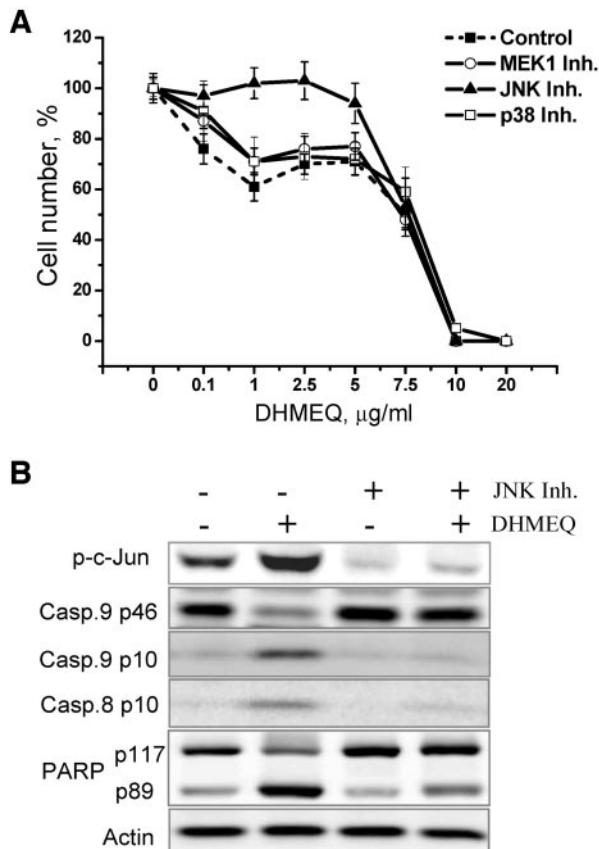


**Fig. 6** Effects of MAPK family inhibitors on DHMEQ cytotoxicity in FRO cells. **A**, Cells plated in 96-well plates were pretreated with 5  $\mu\text{mol/L}$  of each specific inhibitor [MEK1 (PD98059), JNK (SP600125), or p38 (p38 MAPK inhibitor)] for 1 hour then treated with DHMEQ in a range of doses. DMSO at a final concentration of 0.1% was added into the control wells. Plates were incubated for 48 hours, and the cell number was assessed by the water-soluble tetrazolium salt-based assay; bars, mean  $\pm$  SD. **B**, Procaspase and PARP cleavage was analyzed in lysates of cultured cells incubated with 5  $\mu\text{g/ml}$  DHMEQ for 24 hours with or without 5  $\mu\text{mol/L}$  of JNK inhibitor. Casp, caspase.

we show that DHMEQ treatment of ATC cells inhibited the NF- $\kappa\text{B}$  translocation to the nucleus and decreased the levels of several proteins encoded by the  $\kappa\text{B}$ -dependent genes. As a result of DHMEQ treatment, we observed the activation of caspases and apoptosis in cancer cells *in vitro* and *in vivo*.

The mechanism of apoptosis after the NF- $\kappa\text{B}$  inhibition has been largely investigated. It has been shown that NF- $\kappa\text{B}$  activated the group of genes, the products of which suppressed the apoptotic process at the level of caspase activation (2). The family of small IAPs has been shown to play a principal role in the suppression of apoptotic cell death (28, 29). The cIAP-1, cIAP-2, and XIAP can bind and inhibit caspase-3 and caspase-7, thus contributing to tumor cell resistance to cytotoxic agents (30, 31). Accordingly, targeting IAP family members has been shown to induce apoptosis, reduce proliferative potential, and sensitize tumor cells to chemotherapeutic drugs and ionizing radiation (32, 33). Inhibition of IAP expression is, in fact,

one of the proapoptotic mechanisms of chemotherapeutic drugs that target NF- $\kappa\text{B}$  (34). The proapoptotic effect of NF- $\kappa\text{B}$  inhibition has also been attributed to down-regulation of an apoptosis inhibitor Bcl-xL, which is under the transcriptional regulation of NF- $\kappa\text{B}$  (22, 35). However, the changes in expression level of Bcl-xL in thyroid cancer cells treated with DHMEQ were not as prominent as the suppression of IAPs. The similar absence of DHMEQ inhibitory effect on Bcl family proteins was shown in a previous study (13). One of the possible explanations of these observations is that DHMEQ causes a transient NF- $\kappa\text{B}$  inhibition, and p65 DNA binding was restored in 8 to 12 hours after a single-dose treatment. Probably, a more stable inhibition of NF- $\kappa\text{B}$  is necessary to alter the Bcl-xL level substantially. In contrast, even short-time inhibition of NF- $\kappa\text{B}$  nuclear translocation had a marked effect on the expression of IAPs. Thus, our data suggest that down-regulation of IAP proteins by DHMEQ can affect the balance between pro- and antiapoptotic signals in thyroid cancer cells and trigger apoptosis.

In our previous study, we used a small peptide molecule, SN50 (36), to study the effects of NF- $\kappa\text{B}$  inhibition in ATC cells

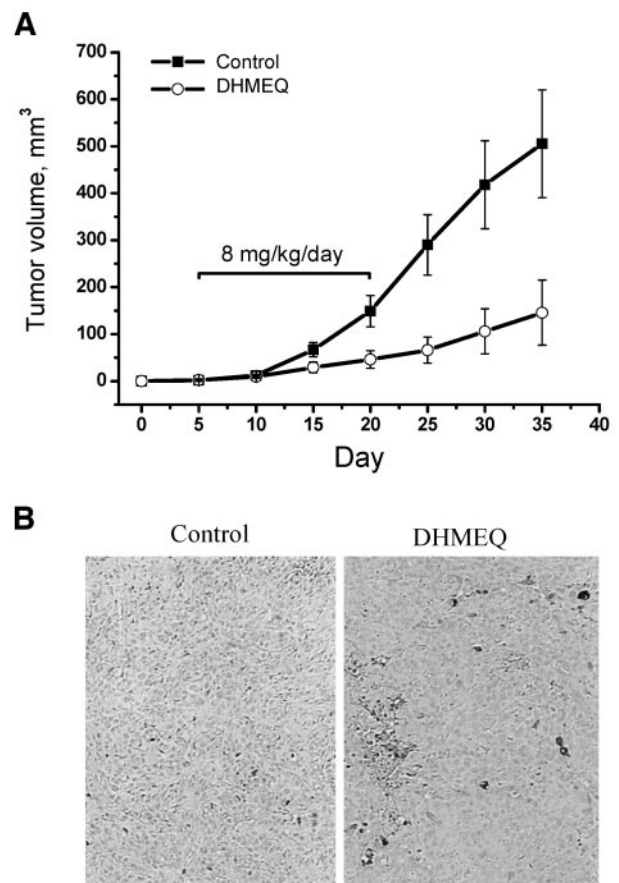


**Fig. 7** Effects of DHMEQ in FRO tumor xenografts grown in athymic mice. DHMEQ, diluted in PBS to DMSO ratio (1:1), was injected i.p. daily at a dose of 8 mg/kg/day for two weeks, beginning from day 5 after tumor implantation. Animals from the control group received a solution of vehicle only. **A**, suppression of tumor growth rate. Bars,  $\pm$  SEM. **B**, manifestation of apoptosis in the tumor tissues after 10 days of DHMEQ treatment. Original magnification,  $\times 100$ .

(10). However, whereas NF- $\kappa$ B inhibition by SN50 substantially retarded cancer cell growth, it did not trigger massive cell death, and only combined treatment with ionizing radiation enhanced cell killing both in culture and *in vivo*. Similar data on adjuvant treatment have been obtained in other solid tumors (37–39). These findings suggested that NF- $\kappa$ B inhibition *per se* did not trigger apoptosis but played an apoptosis-permissive role in cells treated with cytokines, chemotherapeutic drugs, or by ionizing radiation. In the present study, however, DHMEQ inhibited NF- $\kappa$ B signaling at the level of nuclear translocation similarly to SN50 and in parallel induced strong apoptotic cell death in tumor cells. This prompted us to investigate whether DHMEQ could activate additional proapoptotic signaling mechanisms and, hence, initiate apoptotic processes.

JNK activation has been shown to be one of the key proapoptotic factors in mitochondria-dependent death pathways (40), and the duration of this activation is critical for this role of JNK. We have previously shown that in thyroid cancer cells, sustained activation of JNK after exposure to UV correlated with cell death, whereas its transient activation after either X-ray irradiation or induction by growth factors did not (41, 42). In contrast to SN50, which did not activate JNK in the concentrations that inhibited NF- $\kappa$ B nuclear translocation, treatment with DHMEQ induced phosphorylation of JNK1/2 and the downstream transcription factor c-Jun. Prolonged activation of JNK by DHMEQ is likely to be the apoptosis-promoting signal, and JNK activation has been previously shown to be negatively regulated by the NF- $\kappa$ B-induced factors, XIAP and GADD45 $\beta$  (43, 44). Under conditions of altered NF- $\kappa$ B signaling, JNK activity is not inhibited and contributes to apoptosis, and we showed in this study that DHMEQ markedly inhibited NF- $\kappa$ B activity and reduced the levels of factors encoded by the  $\kappa$ B-dependent genes, which may be the mechanism underlying the sustained JNK activation in treated cells. Accordingly, the administration of a specific JNK inhibitor substantially suppressed DHMEQ-induced apoptosis. Thus, our data suggest that JNK activation is necessary to promote apoptosis in thyroid cancer cells in the absence of NF- $\kappa$ B signaling and that the dose range of DHMEQ, within which JNK inhibition prevents cell death, denotes an “apoptotic range” of DHMEQ and correlates with our findings via FACS and procaspase cleavage analysis.

In conclusion, our results show that thyroid carcinoma cells can be effectively killed by a novel NF- $\kappa$ B inhibitor, DHMEQ, both in culture and *in vivo*. The high efficiency of DHMEQ is most likely because of the simultaneous up-regulation of cellular proapoptotic signaling, such as sustained JNK activation and potent inhibition of one of the principal antiapoptotic switches, NF- $\kappa$ B. Our data provide the novel evidence of differential effect of DHMEQ on the tumor cells. At concentrations of up to 1  $\mu$ g/ml (corresponding to about 27  $\mu$ mol/L), DHMEQ can trigger caspase-mediated apoptosis in thyroid carcinoma cells. However, increasing DHMEQ concentrations changes the mechanism of its cytotoxic effects from apoptosis to caspase-independent necrotic-like cell death. We also showed the relative resistance of normal thyroid epithelium to DHMEQ-induced apoptosis, suggesting the preferential targeting of cancer cells. Thus, our study indicates the potential usefulness of DHMEQ in novel treatment strategies for advanced human thyroid cancer.

## REFERENCES

- Barkett M, Gilmore TD. Control of apoptosis by Rel/NF-kappaB transcription factors. *Oncogene* 1999;18:6910–24.
- Wang CY, Mayo MW, Korneluk RG, Goeddel DV, Baldwin AS Jr. NF-kappaB antiapoptosis: induction of TRAF1 and TRAF2 and c-IAP1 and c-IAP2 to suppress caspase-8 activation. *Science (Wash DC)* 1998;281:1680–3.
- Suzuki A, Tsutomi Y, Akahane K, Araki T, Miura M. Resistance to Fas-mediated apoptosis: activation of caspase 3 is regulated by cell cycle regulator p21WAF1 and IAP gene family ILP. *Oncogene* 1998;17:931–9.
- Rayet B, Gelinas C. Aberrant rel/nfkb genes and activity in human cancer. *Oncogene* 1999;18:6938–47.
- Baldwin AS. Control of oncogenesis and cancer therapy resistance by the transcription factor NF-kappaB. *J Clin Invest* 2001;107:241–6.
- Hideshima T, Chauhan D, Richardson P, et al. NF-kappa B as a therapeutic target in multiple myeloma. *J Biol Chem* 2002;28:28.
- Waddick KG, Uckun FM. Innovative treatment programs against cancer: II. Nuclear factor-kappaB (NF-kappaB) as a molecular target. *Biochem Pharmacol* 1999;57:9–17.
- Orlowski RZ, Baldwin AS Jr. NF-kappaB as a therapeutic target in cancer. *Trends Mol Med* 2002;8:385–9.
- Visconti R, Cerutti J, Battista S, et al. Expression of the neoplastic phenotype by human thyroid carcinoma cell lines requires NFkappaB p65 protein expression. *Oncogene* 1997;15:1987–94.
- Starenki D, Namba H, Saenko V, Ohtsuru A, Yamashita S. Inhibition of nuclear factor-kappaB cascade potentiates the effect of a combination treatment of anaplastic thyroid cancer cells. *J Clin Endocrinol Metab* 2004;89:410–8.
- Matsumoto N, Ariga A, To-e S, et al. Synthesis of NF-kappaB activation inhibitors derived from epoxyquinomicin C. *Bioorg Med Chem Lett* 2000;10:865–9.
- Ariga A, Namekawa J, Matsumoto N, Inoue J, Umezawa K. Inhibition of tumor necrosis factor-alpha-induced nuclear translocation and activation of NF-kappa B by dehydroxymethylepoxyquinomicin. *J Biol Chem* 2002;277:24625–30.
- Kikuchi E, Horiguchi Y, Nakashima J, et al. Suppression of hormone-refractory prostate cancer by a novel nuclear factor kappaB inhibitor in nude mice. *Cancer Res* 2003;63:107–10.
- Horiguchi Y, Kuroda K, Nakashima J, Murai M, Umezawa K. Antitumor effect of a novel nuclear factor-kappaB activation inhibitor in bladder cancer cells. *Expert Rev Anticancer Ther* 2003;3:793–8.
- Kurebayashi J, Otsuki T, Tanaka K, et al. Medroxyprogesterone acetate decreases secretion of interleukin-6 and parathyroid hormone-related protein in a new anaplastic thyroid cancer cell line, KTC-2. *Thyroid* 2003;13:249–58.
- Kurebayashi J, Tanaka K, Otsuki T, et al. All-trans-retinoic acid modulates expression levels of thyroglobulin and cytokines in a new human poorly differentiated papillary thyroid carcinoma cell line, KTC-1. *J Clin Endocrinol Metab* 2000;85:2889–96.
- Kawabe Y, Eguchi K, Shimomura C, et al. Interleukin-1 production and action in thyroid tissue. *J Clin Endocrinol Metab* 1989;68:1174–83.
- Li N, Karin M. Signaling pathways leading to nuclear factor-kappa B activation. *Methods Enzymol* 2000;319:273–9.
- Renard P, Ernest I, Houbion A, et al. Development of a sensitive multi-well colorimetric assay for active NFkappaB. *Nucleic Acids Res* 2001;29:E21.
- Pahl HL. Activators and target genes of Rel/NF-kappaB transcription factors. *Oncogene* 1999;18:6853–66.
- Stehlik C, de Martin R, Kumabashiri I, et al. Nuclear factor (NF)-kappaB-regulated X-chromosome-linked iap gene expression protects endothelial cells from tumor necrosis factor alpha-induced apoptosis. *J Exp Med* 1998;188:211–6.
- Chen C, Edelstein LC, Gelinas C. The Rel/NF-kappaB family directly activates expression of the apoptosis inhibitor Bcl-x(L). *Mol Cell Biol* 2000;20:2687–95.

23. Thorburn A. Death receptor-induced cell killing. *Cell Signalling* 2004;16:139–44.
24. Slee EA, Harte MT, Kluck RM, et al. Ordering the cytochrome c-initiated caspase cascade: hierarchical activation of caspases-2, -3, -6, -7, -8, and -10 in a caspase-9-dependent manner. *J Cell Biol* 1999;144:281–92.
25. Makin G, Dive C. Apoptosis and cancer chemotherapy. *Trends Cell Biol* 2001;11:S22–6.
26. Xia Z, Dickens M, Raingeaud J, Davis RJ, Greenberg ME. Opposing effects of ERK and JNK-p38 MAP kinases on apoptosis. *Science (Wash DC)* 1995;270:1326–31.
27. Marshall CJ. Specificity of receptor tyrosine kinase signaling: transient versus sustained extracellular signal-regulated kinase activation. *Cell* 1995;80:179–85.
28. Salvesen GS, Duckett CS. IAP proteins: blocking the road to death's door. *Nat Rev Mol Cell Biol* 2002;3:401–10.
29. LaCasse EC, Baird S, Korneluk RG, MacKenzie AE. The inhibitors of apoptosis (IAPs) and their emerging role in cancer. *Oncogene* 1998;17:3247–59.
30. Roy N, Deveraux QL, Takahashi R, Salvesen GS, Reed JC. The c-IAP-1 and c-IAP-2 proteins are direct inhibitors of specific caspases. *EMBO J* 1997;16:6914–25.
31. Deveraux QL, Takahashi R, Salvesen GS, Reed JC. X-linked IAP is a direct inhibitor of cell-death proteases. *Nature (Lond)* 1997;388:300–4.
32. Holcik M, Yeh C, Korneluk RG, Chow T. Translational upregulation of X-linked inhibitor of apoptosis (XIAP) increases resistance to radiation induced cell death. *Oncogene* 2000;19:4174–7.
33. Hu Y, Cherton-Horvat G, Dragowska V, et al. Antisense oligonucleotides targeting XIAP induce apoptosis and enhance chemotherapeutic activity against human lung cancer cells in vitro and in vivo. *Clin Cancer Res* 2003;9:2826–36.
34. Biswas DK, Martin KJ, McAlister C, et al. Apoptosis caused by chemotherapeutic inhibition of nuclear factor-kappaB activation. *Cancer Res* 2003;63:290–5.
35. Huerta-Yepez S, Vega M, Jazirehi A, et al. Nitric oxide sensitizes prostate carcinoma cell lines to TRAIL-mediated apoptosis via inactivation of NF-kappaB and inhibition of Bcl-x(L) expression. *Oncogene* 2004;23:4993–5003.
36. Lin YZ, Yao SY, Veach RA, Torgerson TR, Hawiger J. Inhibition of nuclear translocation of transcription factor NF-kappa B by a synthetic peptide containing a cell membrane-permeable motif and nuclear localization sequence. *J Biol Chem* 1995;270:14255–8.
37. Wang CY, Cusack JC Jr, Liu R, Baldwin AS Jr. Control of inducible chemoresistance: enhanced anti-tumor therapy through increased apoptosis by inhibition of NF-kappaB. *Nat Med* 1999;5:412–7.
38. Keane MM, Rubinstein Y, Cuello M, et al. Inhibition of NF-kappaB activity enhances TRAIL mediated apoptosis in breast cancer cell lines. *Breast Cancer Res Treat* 2000;64:211–9.
39. Chen S, Fribley A, Wang CY. Potentiation of tumor necrosis factor-mediated apoptosis of oral squamous cell carcinoma cells by adenovirus-mediated gene transfer of NF-kappaB inhibitor. *J Dent Res* 2002;81:98–102.
40. Davis RJ. Signal transduction by the JNK group of MAP kinases. *Cell* 2000;103:239–52.
41. Hara T, Namba H, Yang TT, et al. Ionizing radiation activates c-Jun NH2-terminal kinase (JNK/SAPK) via a PKC-dependent pathway in human thyroid cells. *Biochem Biophys Res Commun* 1998;244:41–4.
42. Shklyayev SS, Namba H, Mitsutake N, et al. Transient activation of c-Jun NH2-terminal kinase by growth factors influences survival but not apoptosis of human thyrocytes. *Thyroid* 2001;11:629–36.
43. Tang G, Minemoto Y, Dibling B, et al. Inhibition of JNK activation through NF-kappaB target genes. *Nature (Lond)* 2001;414:313–7.
44. De Smaele E, Zazzeroni F, Papa S, et al. Induction of gadd45beta by NF-kappaB downregulates pro-apoptotic JNK signalling. *Nature (Lond)* 2001;414:308–13.